

THE OPTICAL FIELD ANGLE DISTORTION CALIBRATION FEASIBILITY STUDY
FOR THE HUBBLE SPACE TELESCOPE FINE GUIDANCE SENSORS

K. Luchetti, G. Abshire, L. Hallock, and R. McCutcheon
Computer Sciences Corporation

ABSTRACT

The results of an analytical study to investigate the feasibility of calibrating the Hubble Space Telescope's (HST's) fine guidance sensors (FGSs) within HST mission accuracy limits are presented. The study had two purposes: (1) to determine the mathematical feasibility of the optical field angle distortion (OFAD) calibration algorithm and (2) to confirm that the OFAD, plate scale, and FGS-to-FGS alignment calibration algorithms produced a calibration of the FGSs that satisfied mission requirements. The study concluded that the mathematical specification of the OFAD algorithm is adequate and permits a determination of the FGS calibration parameters (accurate to better than 0.003 arc-second) sufficient to meet the mission requirements. The algorithms implemented, the characteristics of the simulated data and procedures for data analysis, and the study's results are discussed. In addition, several useful techniques for improving the stability and accuracy of the OFAD solution are outlined.

1. INTRODUCTION

1.1 STUDY BACKGROUND AND PURPOSE

The success of the Hubble Space Telescope (HST) depends critically on the capabilities to accurately place a target in the desired fine guidance sensor (FGS) aperture, precisely control HST pointing, and track moving targets in any FGS aperture. These capabilities depend, in turn, on precise determination of the optical field angle distortion (OFAD), plate scale, and relative alignments of the FGSs. Failure in any of these calibrations means failure to meet HST mission accuracy requirements. Using data as realistic as possible, we conducted a feasibility study to verify that the HST Payload Operations Control Center (POCC) Applications Software Support (PASS) algorithms for these calibrations will, in concert, satisfy mission accuracy requirements.

We performed the study using PASS software implementing the current form of the optical telescope assembly (OTA) calibration algorithms, original versions of which were specified by Perkin-Elmer (P-E) in 1984 (References 1 through 4). The current forms of the algorithms incorporate corrections and enhancements recommended by Computer Sciences Corporation (CSC), Goddard Space Flight Center (GSFC), Marshall Space Flight Center (MSFC), W. Jefferys of the astrometry team, and K. Minka of Computer Technology Associates (CTA). The baselined source specifying the mathematical details of the OTA algorithms is the PASS requirements specification document (Reference 5).

Performance of the feasibility study required the careful coordination of eight separate software functions: data simulation, telemetry processing, data adjustment, plate scale calibration using the calibrated plate method, optical distortion calibration using the mini-OFAD algorithm, plate scale calibration using the moving asteroid method, optical distortion calibration using the P-E-supplied OFAD algorithm, and FGS-to-FGS alignment calibration. We used the PASS attitude data simulator, which was originally developed to test attitude determination software, to generate data for all of the calibration functions studied. Reference 5 provides a detailed description of the simulator's algorithms and capabilities. We used the PASS offline telemetry processor (OTP) to convert the necessary HST FGS data to usable engineering format for the study; Reference 5 provides a detailed description of the OTP.

1.2 ARTICLE OVERVIEW AND TERM/CONCEPT DEFINITION

Section 2 of this article briefly describes the algorithms for the data adjustment and calibration functions analyzed in the OFAD feasibility study. Section 3 outlines the evolution of the OFAD algorithm in response to various problems encountered during OFAD prototype software testing. Section 4 details the data simulation and data reduction activities of the feasibility study; in addition, that section specifies the calibration scenario followed in the study, as well as the original strawman scenario recommended by P-E. Section 5 discusses the results of the study, and Section 6 specifies the conclusions.

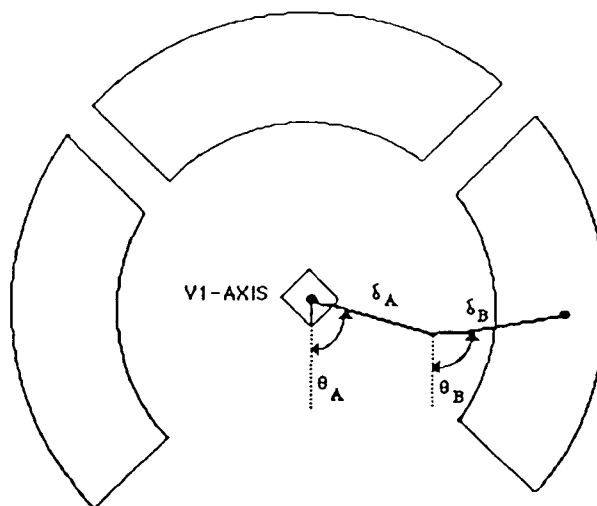
The following paragraphs briefly define terms used and concepts referred to throughout this article:

FGSs -- Each of the HST's three FGSs consists of a system of photomultiplier tubes (PMTs) and amplitude interferometers in white light (Koesters' prism). Because only two

FGSs are required at any particular time for guidance, the third FGS can be used to conduct high-precision astrometric observations.

Image and Object Space -- An image space measurement is the direction of the observed star as measured by the FGS. An object space measurement is the true direction of the observed star. The difference between object and image space measurements is the magnification of the FGS.

Star Selector Deviation and Offset Angles -- Two beam deflectors, called star selectors, rotate to bring light from an object anywhere in the FGS field of view (FOV) into the 5-by-5-arc-second square aperture of the FGS detector assembly. Each of the two star selectors (star selectors A and B) provides a conical scan vector with a diameter of 7.1 arc-minutes in object space. Figure 1 illustrates the star selector deviation and offset angles:



Note:

θ_A and θ_B = star selector A and B deviation angles, respectively
 δ_A and δ_B = star selector A and B offset angles, respectively

Figure 1. FGS Star Selector Deviation and Offset Angles

Distortion Polynomials -- The OFAD algorithm solves for distortion coefficients for use in converting distorted star positions to undistorted star positions in object space. Although the distortion coefficients (also referred to as distorted-to-true coefficients) are not required by any elements of the HST software system except OFAD, the PASS software converts them into coefficients that are used throughout the HST system, as specified below.

<u>Coefficient Type</u>	<u>Used By</u>
Distorted-to-undistorted image space	PASS attitude determination software PASS OTA calibration software
Undistorted-to-distorted image space	PASS mission scheduling software PASS attitude simulation software
Undistorted-to-distorted object space	Onboard flight software (OBC)

Observation Sets and Maneuver Sequence -- Because of the OFAD algorithm's complexity and the large number of parameters solved for in an OFAD execution, the algorithm requires a large quantity of input data (i.e., FGS measurements) to obtain a valid distortion calibration. The HST collects the data by taking FGS measurements of a star field at several different spacecraft attitudes. The measurements of a star field at a specific attitude are referred to as an observation set or frame.

The maneuver sequence for collection of OFAD data consists of 13 pitch-yaw maneuvers and 2 roll maneuvers from a reference attitude. The pitch-yaw maneuvers include nine maneuvers forming an ellipsoid about the reference attitude and four larger offset maneuvers toward the FGS wings. Each observation set consists of approximately 30 stars.

2. BRIEF ALGORITHM DESCRIPTIONS

Calibration of the HST's FGSs involves four major software functions: data adjustment (initial data reduction), plate scale calibration, optical distortion calibration, and FGS-to-FGS alignment calibration. This section briefly describes the algorithms for these functions, which were originally provided by P-E and revised by CSC and P-E as required.

2.1 INITIAL DATA REDUCTION

The purpose of initial data reduction is to read onboard computer (OBC) quaternion and FGS data from the OTA engineering data file (output from the OTP), edit these data to eliminate any irregularities, locate FGS star tracks, and form and identify FGS observation vectors corresponding to these tracks. The primary output from initial data reduction is the OTA prepared data file, which contains the computed FGS image space vectors and

associated information. The OTA prepared data file is the primary input to the OFAD, plate scale, and FGS-to-FGS alignment calibration algorithms.

2.2 PLATE SCALE CALIBRATION

The purpose of plate scale calibration is to compute the scale factor that converts FGS measurements from image to object space. The PASS software currently provides two methods for computing the plate scale: (1) the calibrated plate method and (2) the moving asteroid method. The calibrated plate method uses ground-measured star observations to determine the plate scale. Because this method cannot produce the accuracy required, it serves as an interim technique. The moving asteroid method uses minor planets, specially selected by the astrometry team, that move across the length of the FGS FOV. The use of these planets, whose ephemerides are well known (i.e., to within approximately 0.5 milliarc-second), enables a high level of accuracy in plate scale calibration. In both cases the primary input is the OTA prepared data file produced by the initial data reduction function, and the output is the FGS plate scale.

2.3 OPTICAL DISTORTION CALIBRATION

The purpose of distortion calibration is to compensate for any biases in FGS-measured star directions that cannot be modeled by a rotation (via FGS-to-FGS alignment calibration) or by a scale (via plate scale calibration). P-E models distortion using polynomial functions of the direction cosines, as specified by the following equations:

$$X_U = X_D - \sum_{L,M} a_{LM} X_D^L Y_D^M$$

$$Y_U = Y_D - \sum_{L,M} b_{LM} X_D^L Y_D^M$$

where X_U, Y_U = undistorted X and Y object space direction cosines, respectively

X_D, Y_D = FGS-measured distorted X and Y object space direction cosines,
respectively

a_{LM} = distorted-to-undistorted object space distortion coefficient for the X-polynomial for which the exponent of the X direction cosine is L and the exponent of the Y direction cosine is M

b_{LM} = distorted-to-undistorted object space distortion coefficient for the Y-polynomial for which the exponent of the X direction cosine is L and the exponent of the Y direction cosine is M

The PASS software currently includes two algorithms for calibrating distortion: (1) the method provided by P-E and referred to as the OFAD algorithm and (2) the mini-OFAD algorithm. The mini-OFAD algorithm, the simpler of the two, solves only for the distortion polynomial coefficients, whereas the OFAD algorithm solves for many peripheral parameters, specifically the star direction cosines and the attitude maneuver angles. Because the mini-OFAD algorithm determines fewer parameters than does its more complex counterpart, it requires less FGS data for input. However, the mini-OFAD algorithm must use ground-measured star directions as input when specifying star reference directions; and because the error in the ground measurements is expected to be an order of magnitude higher than the OFAD error budget, the simpler algorithm cannot generate final distortion calibration values. The mini-OFAD algorithm can initialize the OFAD algorithm, which internally computes reference star direction cosines and therefore does not require input of ground measurements. The OFAD algorithm can also solve for offset and deviation angles, a capability that currently is not present in the mini-OFAD algorithm. For both algorithms, the primary input is the OTA prepared data file produced by the initial data reduction function. The user can reject any suspect observation in this file before it is used by the algorithm. Sections 2.3.1 and 2.3.2 describe the two OFAD calibration algorithms in greater detail.

2.3.1 Mini-OFAD Algorithm

The mini-OFAD algorithm calibrates the distortion coefficients using a least-squares procedure (References 6 and 7) that compares the direction cosines of an FGS-measured star field to ground-measured values. The equations of condition are of the form

$$X_D - \sum_{L,M} a_{LM} X_D^L Y_D^M - \left\{ [R_{MINI}] \hat{\xi}_A \right\}_X = 0$$

$$Y_D - \sum_{L,M} b_{LM} X_D^L Y_D^M - \{ [R_{MINI}] \hat{\xi}_A \}_Y = 0$$

where $[R_{MINI}]$ = rotation error matrix

$\hat{\xi}_A$ = differential aberration-perturbed ground-measured star vector rotated into FGS object space

and X_D , Y_D , a_{LM} , and b_{LM} are as defined in Section 2.3. The algorithm generates a pair of equations of condition (X and Y) for each star observation.

The distortion calibration using the mini-OFAD algorithm proceeds as follows. First, the FGS-measured image space direction cosines are transformed to object space (generating the parameters X_D and Y_D for each star observation) using the current plate scale value. Next, the ground-measured background star right ascensions and declinations are transformed to geocentric inertial (GCI) reference frame vectors (GCI coordinates are Earth-centered celestial coordinates), and full velocity aberration effects corresponding to the observation time are applied to the GCI vector. Using the telemetered attitude and the current alignment value, the full velocity aberration-perturbed GCI vector is rotated to FGS object space, yielding the vector $\hat{\xi}_A$, which contains differential velocity aberration perturbations. In the first distortion calibration sequence, the rotation error matrix $[R_{MINI}]$ is initialized to the identity matrix. Using these values for X_D , Y_D , $\hat{\xi}_A$, and $[R_{MINI}]$ and initial estimates for a_{LM} and b_{LM} , updated distortion coefficients are determined to provide the best fit to the equations of condition.

Following convergence (or upon exceeding a maximum number of iterations), an updated value of $[R_{MINI}]$ is determined as follows. Using the updated distortion coefficients, the undistorted FGS-measured direction cosines (X_U and Y_U) are determined using the equations specified in Section 2.3. Least-squares computation of the distortion coefficients followed by q-method calculation of the rotation error matrix is iterated until convergence is achieved or a maximum number of iterations is exceeded. Using the q-method (Reference 8), the rotation matrix $[R_{MINI}]$, which maps the vector $\hat{\xi}_A$ into the undistorted measurement vector, $(X_U, Y_U, Z_U)^T$, is determined. In effect, $[R_{MINI}]$ is an error matrix that corrects for errors in the FGS alignment matrix and telemetered attitude quaternion.

The only output from distortion calibration using the mini-OFAD algorithm is the distortion polynomial coefficients, which are used as initial estimates to the OFAD algorithm and can also be used as input to the other OTA calibration algorithms described in this article.

2.3.2 OFAD Algorithm

The OFAD algorithm calibrates the distortion coefficients, as well as offset and deviation angles, using a least-squares procedure (References 6 and 7) that compares the direction cosines of a star field at several spacecraft attitudes (referred to hereafter as observation sets). A somewhat simplified version of the equations of condition (ignoring terms relative to offset and deviation angle biases) is

$$X_D - \sum_{L,M} a_{LM} X_D^L Y_D^M - \{ [D_A] [R_{MAXI}] \hat{\xi}_T \}_X = 0$$

$$Y_D - \sum_{L,M} b_{LM} X_D^L Y_D^M - \{ [D_A] [R_{MAXI}] \hat{\xi}_T \}_Y = 0$$

where $[D_A]$ = matrix that adds differential velocity aberration at the time of the observation to the "true" star direction vector at the given attitude

$[R_{MAXI}]$ = attitude change Euler angle matrix for transformation from the reference observation set to other observation sets

$\hat{\xi}_T$ = "true" star direction cosines in FGS object space at the reference observation set

and X_D , Y_D , a_{LM} , and b_{LM} are as defined in Section 2.3. The algorithm generates a pair of equations of condition (X and Y) for each star observation.

Distortion calibration using the OFAD algorithm proceeds as follows. FGS-measured image space direction cosines are transformed to object space (generating the parameters X_D and Y_D for each star observation) using the current plate scale value. Initial estimates of the vector $\hat{\xi}_T$ are obtained by removing distortion (using the initial distortion coefficient values) and differential velocity aberration from FGS measurements of star directions at the reference observation set attitude. Initial estimates of $[R_{MAXI}]$ are obtained using the

q-method. The matrix $[R_{MAXI}]$ that transforms the reference observation set to the reference observation set is defined to be the identity matrix. Updated values of $\hat{\xi}_T$ and the Euler angles defining $[R_{MAXI}]$ are determined as part of the least-squares process that determines updated values of the distortion coefficients, along with updated offset and deviation angles. Using these values for $X_D, Y_D, \hat{\xi}_T$, and $[R_{MAXI}]$ and initial estimates for a_{LM} and b_{LM} , updated distortion coefficients, offset and deviation angles, true direction cosines, and attitude change Euler angles are determined to provide a best fit to the equations of condition. The iterative process is continued until convergence is achieved or a maximum number of iterations is exceeded. Once a satisfactory solution is achieved, the final coefficients, offset angle, and deviation angle(s) are output.

2.4 FGS-TO-FGS ALIGNMENT CALIBRATION

The purpose of FGS-to-FGS alignment calibration is to determine the orientation of FGS-1 and FGS-3 relative to FGS-2. FGS-2 defines the HST vehicle reference frame. The primary input is the OTA prepared data file produced by the initial data reduction function, and the output is alignment matrices for transformation from the FGS-1 and FGS-3 frames to the HST vehicle frame.

3. EARLY OFAD PROBLEMS, STUDIES, AND SOLUTIONS

Following our implementation of the basic OFAD algorithm in the prototype software, we began a series of new tests using simulated data corrupted by noise and solving for a broad spectrum of distortion coefficients and offset angle/deviation angle combinations. These tests revealed previously unexpected accuracy, observability, and numerical stability problems. W. Jefferys confirmed many of these problems using his independent software implementation of the OFAD algorithm. Because of the OFAD algorithm's high level of complexity and the difficulties experienced during attempts to solve many of these new problems, GSFC and MSFC decided to create an OFAD technical team to coordinate the efforts of those individuals in the HST community most knowledgeable in the subtleties of the OFAD algorithm. The team, headed by P. Davenport of GSFC, also included F. VanLandingham, G. Abshire, and L. Hallock of CSC; M. Margulies and L. Abramowicz-Reed of P-E; R. Jayroe of MSFC; and W. Jefferys of the University of Texas. The insights of the team into the inner workings of OFAD produced many highly successful enhancements to the original algorithm and resulted in improvements to pre-launch operational procedures and maneuver planning.

This section briefly discusses several of the contributions of the OFAD technical team toward creating a reliable OFAD algorithm.

3.1 OBSERVABILITY AND NUMERICAL STABILITY PROBLEMS

The standard P-E distortion polynomial, consisting of 11 terms in each axis, has the form

$$\begin{aligned} \sum_{L,M} a_{LM} X_D^L Y_D^M = & a_{1,0} X_D + a_{2,0} X_D^2 + a_{1,1} X_D Y_D + a_{0,2} Y_D^2 + a_{3,0} X_D^3 \\ & + a_{2,1} X_D^2 Y_D + a_{1,2} X_D Y_D^2 + a_{0,3} Y_D^3 + a_{5,0} X_D^5 \\ & + a_{3,2} X_D^3 Y_D^2 + a_{1,4} X_D Y_D^4 \end{aligned}$$

$$\begin{aligned} \sum_{L,M} b_{LM} X_D^L Y_D^M = & b_{0,1} Y_D + b_{2,0} X_D^2 + b_{1,1} X_D Y_D + b_{0,2} Y_D^2 + b_{3,0} X_D^3 \\ & + b_{2,1} X_D^2 Y_D + b_{1,2} X_D Y_D^2 + b_{0,3} Y_D^3 + b_{0,5} Y_D^5 \\ & + b_{2,3} X_D^2 Y_D^3 + b_{4,1} X_D^4 Y_D \end{aligned}$$

where a_{LM} , b_{LM} , X_D , and Y_D are as defined in Section 2.3. Most of the early "perfect" data tests (i.e., tests with simulated data uncorrupted by noise) executed using the OFAD prototype software and data generator studied only a subset of the full 11-term polynomial, specifically the 3 quadratic and 4 cubic coefficients. The next step in the algorithm test procedure was to expand the scope of the tests to include linear and fifth-order coefficients. These tests produced algorithm failures centering on the inability of the software to invert the large matrices (having dimensions greater than 100) used in the least-squares calculations.

In the case of the linear coefficients, the inversion problem had two causes. First, we determined empirically in testing that unless roll maneuvers were included in the OFAD maneuver sequence (nominally the simulated data included two observations sets consisting of a +10-degree roll and a -10-degree roll from the reference attitude), no linear coefficients could be determined. Jefferys confirmed this finding analytically and soon afterward modified the planned OFAD observing sequence to include two pure roll maneuvers. The

second anomaly discovered during testing was that the $a_{1,0}$ and $b_{0,1}$ coefficients (linear terms), when taken together, contain a plate scale component, which is not observable by the OFAD algorithm. The initial solution to this problem was to hold the $b_{0,1}$ coefficient constant and solve for only the $a_{1,0}$ coefficient. A later enhancement (discussed in Section 3.3) constrained the solved-for distortion polynomial's $a_{1,0}$ and $b_{0,1}$ coefficients from having a scale component and thereby permitted solving for both linear coefficients. The $a_{0,1}$ and $b_{1,0}$ coefficients (linear cross-terms), when taken together, contain a rotation component, which is not observable by the OFAD algorithm. To solve for the linear cross-terms, the required procedure at that time was to hold the $b_{1,0}$ coefficient constant while solving for the $a_{0,1}$ coefficient. (The current implementation of both the mini-OFAD and OFAD algorithms allows the user to select any polynomial up through fifth order, with a default to the P-E 11-term polynomial.) A later enhancement (discussed in Section 3.3) constrained the solved-for distortion polynomial's $a_{0,1}$ and $b_{1,0}$ coefficients from having a rotation component and thereby permitted solving for both linear coefficients.

Numerical underflow produced the matrix inversion problems in solving for fifth-order coefficients. We solved this problem by adding numerical scaling parameters to the calculations. With appropriately selected values, these parameters provide adequate underflow protection and eliminate a purely numerical source of instability.

3.2 NOISE-CORRUPTED DATA PROBLEM

The effect of corrupting data with noise was the most difficult of all the OFAD problems to solve. Efforts to solve this problem resulted in the enhancement of the original OFAD algorithm with constraints and led to the creation of the mini-OFAD algorithm (Section 3.4). We discovered the problem during our first tests with simulated data corrupted by noise. With perfect data the OFAD algorithm could solve for the "true" distortion polynomial coefficients (i.e., the coefficients simulated in the data generator) to a precision of eight significant figures, even with a very poor initialization. However, with the addition of noise, the effective difference between a solved-for coefficient and the corresponding true value of the coefficient appeared to be one to two orders of magnitude higher than the noise in the data. To determine more quantitatively the size of the discrepancy, we coded a small prototype software utility (called the goodness-of-fit utility). This utility revealed that the resulting error in the undistorted vector computed using the solved-for coefficients was between 60 and 100 times the noise. We therefore referred to the anomaly as "noise magnification."

Jefferys explained the nature of the noise magnification effect empirically (Reference 9), and Davenport explained it analytically (References 10 and 11). Jefferys analyzed the difference between expected and solved-for values and demonstrated that the error could be modeled by an affine transformation (linear translations plus rotation). After removal of the affine fit, the remaining errors were approximately the same size as the original noise. Davenport demonstrated analytically that over the small FOV of an FGS, without input ground measurements to constrain the solution, the polynomial solution could be expected to acquire undesired affine terms. Soon afterward, Davenport further refined his result by proving that the dominant error term can be characterized by a similarity transformation, i.e., a combination of translations in X and Y, a rotation about Z, and a change in plate scale. Jefferys also observed this empirically (Reference 12). The OFAD algorithm can observe none of the four components of a similarity transformation. However, determination of the combined translations and rotations, at least in a relative sense, is possible via FGS-to-FGS alignment calibration (Section 2.4), and, of course, determination of the change in plate scale is possible via plate scale calibration (Section 2.2). It was clear that unless the undesired similarity terms could be kept out of the polynomial solution, the only way to verify the accuracy of the OFAD solution would be to undertake a massive simulation effort in which a complete set of FGS calibration parameters (distortion coefficients, plate scales, and FGS-to-FGS alignments) would be determined for each FGS with highly realistic simulated data, following which the overall accuracy of the complete parameter set would be evaluated. Even if such a simulation indicated that the overall accuracy of the whole parameter set met mission requirements, the necessity of relying on an OFAD algorithm that under operational conditions would displace the solved-for distortion coefficients from the initial values by a large, unpredictable similarity transformation was clearly undesirable.

To alleviate this problem, Davenport recommended introducing four constraints on the OFAD state vector that he believed would inhibit formation of the observed similarity transformation between the solved-for distortion coefficients and the truth (Reference 13). The effect of the constraints was to prohibit the solved-for true direction cosines from picking up similarity terms that could be passed on to the solved-for distortion polynomial. Because no constraint features existed in the original OFAD formulation, the software was enhanced with the new equations specified by Jefferys (Reference 14) and Abramowicz-Reed (Reference 15) incorporating Davenport's constraints in OFAD. Section 3.3 discusses the results of our tests using OFAD software containing this constraint capability.

Finally, the technical team made tentative plans to carry out a full-scale simulation to test the validity of the combined OFAD, plate scale, and alignment calibration solutions in the event that the results of the upcoming tests on the enhanced OFAD algorithm did not prove unambiguously successful. In particular, CSC and P-E began identification and specification of a complete set of biases and physical effects required for generation of realistic simulated data.

3.3 INITIAL ESTIMATES FOR CONSTRAINTS

After implementing in prototype software Davenport's constraints on the solved-for reference observation set star direction cosines (Section 3.2), we began testing the enhanced algorithm with a variety of input polynomials. We determined that the constrained version of the OFAD algorithm, unlike the unconstrained version, was highly sensitive to the accuracy of the distortion coefficient initialization values. The cause of the problem was that the values of the reference direction cosines used to initialize the OFAD least-squares process were determined by removing distortion (using the initial estimates of the coefficients) from FGS measurements of star directions at the reference attitude. Because these initial values of the direction cosines were used to constrain the solved-for values of the direction cosines, once an error was induced in the direction cosines (via the initial coefficient estimates), the algorithm could not recover from the error. As a result, the OFAD algorithm tended to converge to a polynomial solution very close to the initial estimates. In particular, if the OFAD algorithm was initialized with a polynomial having different similarity properties than the "true" polynomial, the effect of the constraints would be to prohibit the OFAD algorithm from solving for the truth.

Soon afterward, Davenport discovered the highly data-dependent nature of the OFAD polynomial's similarity component (References 16 and 17). Therefore, even if the development of undesirable similarity transformations when solving for distortion coefficients could be prohibited, the solved-for coefficients could appear to have nonzero similarity terms when applied to other data. This result emphasized further that tests of the validity of the OFAD algorithm performed in isolation from the plate scale and alignment algorithms would not be reliable, and therefore a full-scale simulation of all three algorithms was required to demonstrate feasibility.

Two approaches to the constraint initialization problem developed. First, CSC recommended that a simpler, more stable form of the OFAD algorithm, a mini-OFAD algorithm

using ground-based data (Section 2.3.1), be developed in the hope that it could be used to detect at an early stage any large biases in the prelaunch distortion coefficient estimates and also be used to provide a more accurate initialization of the full OFAD algorithm. Section 3.4 describes the results of our tests using the mini-OFAD algorithm. The second approach to the constraint initialization anomaly was Davenport's continuing efforts to improve on the existing constraint formulation. Section 3.4 also discusses the new constraints he developed and their applicability to both the mini-OFAD and OFAD algorithms.

3.4 ALIGNMENT/ATTITUDE ERRORS IN MINI-OFAD ALGORITHM

The mini-OFAD algorithm iterates between the least-squares computation of the distortion polynomial coefficients and the q-method calculation of a rotation error matrix. The algorithm can perform the q-method calculation either before or after the least-squares calculation of the distortion polynomial, at user option. Initially, we conducted algorithm tests with data-generator-produced input data that were corrupted by noise but contained no alignment bias. When performing the least-squares calculation of the coefficients prior to computing the rotation error matrix, the mini-OFAD algorithm determined coefficients to an accuracy comparable with the amount of noise in the data and the error in the ground-measured background stars. When the order was reversed, the rotation matrix determination picked up any rotational differences in similarity terms between the initial values of the distortion coefficients and the true values of the distortion coefficients, resulting in a poor solution. Therefore, for the first series of tests, as long as error matrix determination followed coefficient calculation, the mini-OFAD algorithm performed well enough to provide early bias detection capability and an accurate initialization for the OFAD algorithm. However, the addition of a simulated alignment bias (operationally, for mini-OFAD, an apparent alignment bias could be generated by an alignment or attitude error) resulted in undesirable coefficient perturbation. So although the mini-OFAD algorithm was rather insensitive to noise, it unfortunately was highly sensitive to alignment biases or attitude errors, neither of which was a problem to the OFAD algorithm, which uses such information only for aberration calculations.

Davenport's modified constraints (Reference 18) provided the solution to the problems of both algorithms. In his new constraint formulation, the distortion coefficients were constrained such that the similarity content of the distortion polynomial was required to remain the same through all iterations of the OFAD algorithm. When applied to the mini-OFAD algorithm, the constraints prohibited the coefficients from picking up an alignment bias

and/or attitude error. When applied to the OFAD algorithm, the constraints prevented the coefficients from modifying the similarity terms to provide a better fit to the noise. Initially the constraints used fixed points outside the FGS FOV to maintain a constant similarity content. However, because of the data-dependent nature of the similarity components, the use of actual measurement points as input to the constraints produced better results. All OFAD and mini-OFAD runs performed in the feasibility study constrained the distortion polynomial with measured star direction cosines. Implementation of Davenport's new constraints in both OFAD algorithms constituted the last major software enhancement required to support the combined simulation effort.

4. FEASIBILITY STUDY

From February through July 1987, we conducted a feasibility study to test the combined accuracy of FGS calibration parameters determined with the OFAD, plate scale, and FGS-to-FGS alignment calibration software. The study required the simulation of a massive quantity of FGS data that realistically modeled all conceivable sensor biases, telemetry characteristics, and physical phenomena that could affect the in-flight calibration of the FGSs. In addition, the unique characteristics of the FGSs and the unusually high accuracy requirements placed on the calibration process necessitated considerable effort to determine a successful operational scenario for utilizing available software calibration tools. This section provides a detailed account of these activities.

4.1 DATA SIMULATION AND DATA REDUCTION ACTIVITIES

The OFAD feasibility study used a modified version of the PASS attitude simulation software that enabled the realistic simulation of the most important aspects of the HST's FGSs.

4.1.1 Simulation Procedure

Our procedure for generation of data for the full-scale simulation was as follows. First, the PICKLES program, developed by W. Jefferys, was executed to select an appropriate cluster of stars for each observation set being simulated. Capabilities provided by this program included shifting the FGS FOV and deleting any undesirable stars in the FOV. Input to this program was the NGC 188 star catalog; output was the right ascension, declination, and magnitude of each star chosen for the specific observing sequence. Using the MAC Terminal utility program and the VAX screen editor, the output data file from PICKLES was

transferred from the Macintosh personal computer on which the program had been executed to the VAX 11/785; the file was then used as input to a utility program (developed especially for the simulation) for creation of a NAMELIST for use by the PASS simulation software.

Next, the simulator was executed to simulate the attitude profile (defining parameters that have a first-order dependence on attitude) for the observation set and to create astrometry and guide star files, and the data generated were used as input to the attitude simulator for creation of OTA telemetry data. All attitude simulator executions were in batch mode; all other executions were in interactive mode. The telemetry data generated were then used as input to the PASS OTP for creation of an engineering data file. The engineering data file contains attitude quaternion data, fine mode PMT counts, star selector angle data, and engineering data status flags.

The OTA initial data reduction software (IDR) was executed to reduce the engineering data file to the OTA prepared data file, and the prepared data file was then used as input to the plate scale, mini-OFAD, OFAD, and FGS-to-FGS alignment calibration software. Finally, all data created prior to initial data reduction were written to tape.

4.1.2 Errors and Biases

Each type of error and the magnitude of each error to be simulated were specified jointly by CSC and P-E and then submitted to the OFAD technical team for comment. The major sources of the errors simulated were as follows: initialization in the attitude simulator of the distortion coefficients, plate scale values, offset and deviation angles, and FGS alignments; FGS measurements; HST dynamics; and ground measurements of the star positions.

The distortion polynomial used in the attitude simulator executions was a 17-term undistorted-to-distorted image space polynomial specified by P-E. The distortion polynomial used in the IDR executions was a modified version of an 11-term polynomial provided by P-E; the distorted-to-undistorted object and image space coefficients used were identical to those specified by P-E except for the X linear term in the X-polynomial and the Y linear term in the Y-polynomial, which were modified to remove the effects of scale and rotation.

The P-E-specified discrepancy of no more than ± 2 percent in simulator versus IDR plate scale values was adhered to in the simulation. The errors simulated in plate scale values were between 1.0 and 1.4 percent depending on the FGS involved. Errors were also introduced into the deviation and offset angles.

The discrepancies in alignment were computed using small-angle approximation. The error in FGS-1 was computed with a pitch of 1.5 arc-seconds, a roll of -295 arc-seconds, and a yaw of -0.5 arc-second. In both the simulator and IDR executions, FGS-2 and FGS-3 had the same alignment.

The FGS measurements were the second most important source of errors in the simulation. The FGS fine error signal consists of measurements of the number of photons selected by four PMTs and so is subject to Poisson statistics as specified by the square root of the number of photons detected. The two sources of error in star selector angle measurement were the 7-bit correction and the 14-bit correction. These corrections are due to mechanical encoder errors. Both corrections were simulated. Only the 7-bit correction was compensated for in the OTP to within ± 0.32 milliarc-second. The 14-bit correction is a time-independent, low-frequency correction to the star selector angles of about 0.5 arc-second that is not compensated for by the IDR or the OTP. However, because this is a low-frequency correction, it can be compensated for using the distortion coefficients. All of the fine error signals were adjusted for a background with the amount of light generated by a 20th-magnitude star in addition to the expected star.

An HST attitude error of 3 milliarc-seconds due to jitter was simulated, but no error due to uncompensated rate gyro assembly drift was included. The stars in the guide star and astrometry header data files generated by the profile simulator had random position errors of 15 milliarc-seconds from their true locations in the sky.

4.1.3 Data Quantity

The full-scale data simulation was a massive effort requiring heavy use of computer resources. For a single FGS, 17 observation sets were required for distortion coefficient determination, 1 simulator execution was required for mini-OFAD calibration, and 3 simulator executions were required for plate scale calibration. An additional 10 executions were required for FGS-to-FGS alignment calibration, for a grand total of 73. Each observation set consisted of about 40 minutes of simulated data, for a total of

2,920 minutes, or 4.9 hours. We used the observing sequence described in Section 1.2 for the OFAD calibration.

4.2 DATA ANALYSIS SCENARIOS

Because each of the three FGS calibration functions (OFAD, plate scale, and FGS-to-FGS alignment calibration) requires as input the output of the other two, an iterative procedure among the three software modules is required to generate an FGS calibration parameter set that meets the HST mission accuracy requirements.

4.2.1 Strawman Scenario

To provide a starting point for the feasibility study, P-E prepared a preliminary procedure for calibrating the FGSs (Reference 19). This procedure was as follows:

1. Excluding the fifth-order distortion coefficients, iterate between the calibrated plate method for plate scale calibration and the mini-OFAD algorithm for distortion calibration until the change in the plate scale on successive iterations falls to below 0.002 percent.
2. Perform a preliminary alignment calibration.
3. Solving for the full 11-term polynomial, iterate between the OFAD algorithm for distortion calibration and the moving asteroid method for plate scale calibration until convergence is achieved.
4. Calibrate the FGS-to-FGS alignment.
5. Iterate among the OFAD algorithm for distortion calibration, the moving asteroid method for plate scale calibration, and FGS-to-FGS alignment calibration until the alignment matrix changes on successive iterations by less than 0.2 percent.

In the course of performing the feasibility study, we discovered that a number of improvements to the strawman scenario could be made. Section 4.2.2 describes the final calibration procedure used in the study.

4.2.2 Final Operational Scenario

Using the P-E strawman scenario as a starting point, we gradually refined the scenario to improve the accuracy and stability of the solution. The final procedure is described below.

First, as in the P-E scenario, an iterative procedure between the calibrated plate method for plate scale calibration and the mini-OFAD algorithm for distortion calibration was performed until the change in the plate scale on successive iterations fell to below 0.002 percent. In practice, this convergence condition required four executions of the plate scale software and three executions of the mini-OFAD calibration software. In each execution of the mini-OFAD calibration software, three iterations between the least-squares computation of the coefficients and the q-method computation of the rotation error matrix were performed. In the least-squares distortion coefficient computation, three to six iterations were usually performed (on the third cycle with the q-method, at least six iterations were always performed). As in the P-E scenario, no fifth-order coefficients were solved for. In earlier test results, the solution appeared to be somewhat unstable when fifth-order coefficients were included. Because the initial estimates of the linear coefficients ($a_{1,0}$ in the X-polynomial and $b_{0,1}$ in the Y-polynomial) did not satisfy Davenport's constraint for these terms (Reference 18), both linear coefficients could not be determined (using this constraint) without displacing the coefficients from their initial values by a large amount. Instead, the $a_{1,0}$ coefficient in the X-polynomial was determined, whereas the $b_{0,1}$ coefficient in the Y-polynomial was held constant. The remaining coefficients (i.e., the three quadratic and four cubic coefficients) in the standard 11-term polynomial were determined.

After the iterative procedure between the calibrated plate method and the mini-OFAD algorithm converged, a preliminary alignment was determined. Because a complete set of FGS calibration parameters was then available, the goodness-of-fit utility was executed. Of course, in a real operations situation, where the truth is unknown, the goodness-of-fit utility is not usable. The preliminary alignment was used for accuracy checking only; it was not used to initialize the OFAD algorithm or the moving asteroid method. The output from the calibrated plate method and the mini-OFAD algorithm were, however, used to initialize the moving asteroid method and the OFAD algorithm.

Next, an iterative procedure between the moving asteroid method and the OFAD algorithm was performed until convergence was achieved. The convergence criterion selected was that the change in the plate scale on successive iterations be no more than 0.00001 percent.

In a departure from the P-E approach, an asteroid plate scale was determined to initialize the OFAD algorithm. For the OFAD algorithm executions, the full set of 11-term polynomial coefficients, except for the $b_{0,1}$ coefficient in the Y-polynomial, were determined. As in the case of the mini-OFAD algorithm executions, the $b_{0,1}$ coefficient in the Y-polynomial was held constant to avoid a conflict with the requirements of the associated constraint. Also, the B deviation angle and the B offset angle were determined. Solving for more than one deviation or offset angle in a single execution resulted in erratic displacements of the solved-for direction cosines (Section 5.1). Satisfaction of the convergence criterion required four executions of the moving asteroid plate scale calibration software and three executions of the OFAD algorithm. In one execution of the OFAD algorithm, six iterations were usually performed. At the end of each plate scale calculation using the moving asteroid method, the most recent OFAD algorithm and moving asteroid plate scale solutions were checked for consistency using the mini-OFAD algorithm. Unlike the goodness-of-fit utility, the mini-OFAD algorithm can be used to check the consistency of the OFAD algorithm solutions even in an operational setting. However, the goodness-of-fit utility was used in the feasibility study to check the accuracy of the OFAD algorithm solutions on an intermittent basis. The last step of the scenario was to perform an alignment calibration. It was determined that because the OFAD algorithm and the moving asteroid method are relatively insensitive to alignment errors, no iteration among the OFAD algorithm, the moving asteroid method of plate scale calibration, and FGS-to-FGS alignment was required. The final parameter set was consistency checked with the mini-OFAD software and accuracy checked with the goodness-of-fit utility.

5. RESULTS OF FEASIBILITY STUDY

In addition to achieving the study's primary objective of demonstrating feasibility, we also discovered many useful techniques for improving the stability and accuracy of the OFAD solution.

5.1 QUALITATIVE RESULTS

The feasibility study provided an excellent opportunity to test the behavior of the OTA algorithms using realistically simulated data with different combinations of state vector element sets and constraints. The most important discovery was the high sensitivity of both the mini-OFAD and OFAD algorithms to bad data points. As part of the simulation, a star observation was produced with an erroneous 14-bit correction and a consequent error of

approximately 0.5 arc-second. Even using the mini-OFAD algorithm, which is more stable than the OFAD algorithm, this single bad data point out of 38 data points resulted in a level of data degradation sufficient to produce an unacceptably high error in the solved-for polynomial. Considerable effort was required during the study to detect and identify bad data points. In response to this problem, we proposed the enhancement of all the OTA algorithms to include a more sophisticated data validation capability and a series of statistical summary displays to display the vector of conditions and other large arrays. Such summary displays would identify which stars/observation sets constitute the poorest fit to the current distortion polynomial values without requiring the operator to page through an impractically large number of array elements and visually identify the outliers. These enhancements were implemented in the PASS OFAD software after the completion of this study.

One expected problem experienced during the study was some instability when solving for fifth-order coefficient values. To minimize the impact of the instability, the fifth-order terms were held constant in the mini-OFAD algorithm. This helped the mini-OFAD algorithm solve for stable, accurate polynomial coefficients. Having been initialized with a reliable distortion estimate, the OFAD algorithm had no difficulty solving for the fifth-order terms when a higher accuracy solution was required. We believe that some additional improvement could be achieved if better numerical scaling of the coefficients were added to the OFAD algorithms. The improvement of the numerical scaling is currently being studied.

We observed a new, unexpected instability in the first set of mini-OFAD algorithm executions. All the solved-for distortion coefficients (one linear in the X distortion polynomial, three quadratic in X and three in Y, and four cubic in X and four in Y) moved by unrealistically large amounts from their initial estimates during the first least-squares computation before the Euler angle calculation with the q-method. This effect was most observable in the linear term and was amplified when, in test executions, fifth-order terms were determined. Upon recomputation of the coefficients following Euler angle calculation, considerable recovery of the solution occurred, although a larger-than-expected displacement of the solution from the initial estimates remained. Further, but not complete, recovery was achieved on iteration with the plate scale calibration software and upon refinement with the OFAD algorithm. There is currently no explanation for this phenomenon, but this particular instability apparently (on the basis of the calculated accuracy of the solution (Section 5.2)) caused no lasting damage.

We executed the OFAD algorithm numerous times to solve for different combinations of offset and deviation angles. The more parameters solved for, the greater the displacement of the solved-for star direction cosines from their initial estimates. In solving for two deviation angles and one offset angle, the shift in the star direction cosines was as much as 1 arc-second even though the accuracy of the mini-OFAD distortion estimate was expected to be no worse than about 20 milliarc-seconds. The standard parameter set was one deviation angle and one offset angle. For such cases the maximum displacement of direction cosines was between 0.2 and 0.5 arc-second. Although no degradation in the achieved accuracy was observed (Section 5.2), such a large movement in the star field is quite unsettling. The reason for the displacement could be nonutilization (during the feasibility study) of the old constraints on the direction cosines (Section 3.2). These constraints might, in conjunction with the new constraints on the coefficients used during the study (Section 3.4), provide for an accurate, stable solution without unrealistic displacement of the state vector's non-calibration elements. Since completion of the study, the additional four constraints have been added to the PASS OFAD software.

5.2 QUANTITATIVE RESULTS

The primary reason for conducting this study was to determine if, with a proper operational scenario, the three FGS calibration algorithms (plate scale, OFAD, and FGS-to-FGS alignment calibration) could determine an FGS calibration parameter set of sufficient accuracy to meet HST mission requirements. As shown in Table 1, for the standard 11-term polynomial case, the accuracy of an FGS relative to itself (i.e., the combined accuracy of plate scale and OFAD parameters) was always below 1.5 milliarc-seconds, as against an accuracy requirement of 3 milliarc-seconds. The accuracy of either FGS-1 or FGS-3 relative to FGS-2 (i.e., the combined accuracy of the plate scale, OFAD, and alignment parameters) was less than 3 milliarc-seconds, as against an accuracy requirement of 5 milliarc-seconds. Furthermore, the error in inverting the solved-for polynomial for onboard use was negligible. These results are outstanding and provide good reason for optimism about the probability for success of the in-flight calibration activity.

Results achieved using a 17-term polynomial (adding in the linear cross-term and the 5 fourth-order terms) were similar to the 11-term polynomial results, with one major exception. The inversion error when transforming a 17-term distorted-to-undistorted object space polynomial to an 11-term undistorted-to-distorted object space polynomial was much higher than when inverting the 11-term distorted-to-undistorted object space polynomial.

Table 1. OFAD and Mini-OFAD Algorithm Accuracies

CONDITIONS	Mean FGS-1 (mas)			Mean FGS-2 (mas)		Mean FGS-3 (mas)		
	wrt FGS-1	wrt FGS-2	Inversion	wrt FGS-2	Inversion	wrt FGS-3	wrt FGS-2	Inversion
OFAD: 17 TERMS, θ_B, δ_B	1.0 ± 0.8	2.0 ± 1.4	1.2 ± 1.0	0.5 ± 0.4	1.2 ± 1.2	1.7 ± 0.9	2.5 ± 1.8	7.7 ± 5.5
OFAD: 11 TERMS, θ_B, δ_B	0.8 ± 0.7	2.3 ± 1.7	0.03 ± 0.01	0.7 ± 0.7	0.02 ± 0.01	1.1 ± 0.7	2.1 ± 1.6	0.04 ± 0.02
MINI-OFAD: 17 TERMS	10.3 ± 14.0	N/A	3.0 ± 3.4	5.3 ± 4.1	2.3 ± 1.5	21.8 ± 16.9	N/A	13.5 ± 8.0
MINI-OFAD: 17 TERMS	9.8 ± 10.5	N/A	0.07 ± 0.04	4.0 ± 3.3	0.10 ± 0.06	37.1 ± 29.5	N/A	0.61 ± 0.47

NOTE: mas = milliarc-second
wrt = with respect to
N/A = not applicable

For FGS-3, the inversion error was greater than the total error budget. We determined the major contributor to the inversion error to be the linear cross-term. Provided the distortion encountered in flight contains no components that are best modeled by linear cross-terms, solving for the standard 11-term polynomial in flight should be no problem.

Table 1 also specifies the accuracies of the mini-OFAD solutions (in conjunction with asteroid-method-computed plate scales) used to initialize the OFAD algorithm computations. For FGS-1 and FGS-2, the accuracy of the calibration of the FGS relative to itself was about 10 milliarc-seconds or better. Because the expectation had been that the mini-OFAD algorithm would calculate distortion coefficients accurate to about 20 to 30 milliarc-seconds (largely due to error in the reference vectors), the accuracies achieved with FGS-1 and FGS-2 were surprisingly good. In fact, for FGS-2, the accuracies with the mini-OFAD algorithm almost met the 3-milliarc-second mission requirement. For FGS-3, the accuracies (relative to FGS-3) were much worse, due to the presence of additional bad simulated data points. However, even with FGS-3, the approximate distortion values supplied by the mini-OFAD algorithm provided the OFAD algorithm with a sufficiently accurate initialization to allow the latter to compute coefficients accurate to better than 3 milliarc-seconds. In addition, the errors experienced when inverting mini-OFAD solutions followed the same pattern as with OFAD solutions, i.e., the inversion errors for the 11-term polynomial were small, but the errors for a 17-term polynomial were unacceptably large.

6. CONCLUSIONS

We believe that our study of FGS calibration accuracy demonstrates that the current versions of the PASS plate scale, OFAD, and FGS-to-FGS alignment calibration algorithms are capable of meeting the HST mission's very stringent accuracy requirements, provided the actual distortion encountered in flight can be represented with the current P-E 11-term polynomial. In particular, it is essential that the distortion encountered in flight not contain any components best modeled by linear cross-terms, because no such terms are present in the current 11-term model. Should any linear cross-terms or other important, unrepresented terms be present, the PASS software has the capability to solve for a larger polynomial including the extra terms, but the flight software's inverse polynomial is limited to 11 terms. The study did not obtain an accurate inversion from a larger, more general polynomial to the standard 11-term polynomial within accuracy limits. Therefore, to the extent that the distortion simulated in this study resembles the real distortion that will be encountered in flight, the study shows the OFAD algorithm to be adequate to support HST launch.

CSC acknowledges the valuable assistance of the OFAD technical team, headed by P. Davenport of GSFC, in determining the initial parameter values for this study and in interpreting the study's results. Other non-CSC members of the team include R. Jayroe of MSFC, L. Abramowicz-Reed and M. Margulies of P-E, and W. Jefferys of the University of Texas. Also, CSC extends thanks to W. Lindboe and W. Ruml of CSC for program runs made in support of the simulation activities for this study.

CSC performed the OFAD calibration feasibility study in support of contract NAS 5-26685.

REFERENCES

1. L. Abramowicz-Reed, "Space Telescope Plate Scale Calibration Algorithm," Memorandum ST-SE-3360, Perkin-Elmer, April 2, 1984
2. G. Dente and L. Abramowicz-Reed, "Space Telescope Optical Field Angle Distortion Calibration Algorithm," Memorandum ST-SE-3336, Perkin-Elmer, March 23, 1984
3. Perkin-Elmer, PR-1011, Algorithms for Fine Guidance Sensor/V1, V2, V3 Alignment (Part 1) and Fine Guidance Sensor/Scientific Instrument Alignment (Part 2), December 7, 1984
4. --, PR-1005, Initial Data Reduction Techniques for Star Selector Positions, December 7, 1984

5. Computer Sciences Corporation, CSC/TM-82/6045, Space Telescope POCC Applications Software Support (PASS) Requirements Specification (Revision E), September 1987
6. W. Jefferys, "On the Method of Least Squares," The Astronomical Journal, February 1980, vol. 85, no. 2, pp. 177- 181
7. --, "On the Method of Least Squares II," The Astronomical Journal, January 1981, vol. 86, no. 1, pp. 149-155
8. Computer Sciences Corporation, CSC/TM-77/6034, Analysis of Least-Squares Attitude Determination Routine, DOAOP, February 1971
9. W. Jefferys, Attachment to Minutes of May 1, 1986, OFAD Technical Meeting, May 12, 1986
10. P. Davenport, "Deficiency of Linear Distortion Coefficients in OFAD," Memorandum, National Aeronautics and Space Administration, Goddard Space Flight Center, May 19, 1986
11. --, "Analysis of OFAD Noise Problem," Memorandum, National Aeronautics and Space Administration, Goddard Space Flight Center, May 30, 1986
12. W. Jefferys, "Why Only Four Constants?," Memorandum, University of Texas at Austin, May 30, 1986
13. P. Davenport, "The OFAD Noise Problem, A Review and the Solution," Memorandum, National Aeronautics and Space Administration, Goddard Space Flight Center, June 25, 1986
14. W. Jefferys, "Constraints in OFAD," Memorandum, University of Texas at Austin, July 9, 1986
15. L. Abramowicz-Reed, Memorandum on OFAD Constraints, P-E, August 12, 1986
16. P. Davenport, "Additional Problems With Polynomial Representing Distortion," Memorandum, National Aeronautics and Space Administration, Goddard Space Flight Center, October 3, 1986
17. --, Attachment to Minutes of October 2, 1986, OFAD Technical Meeting, November 5, 1986
18. --, "Modification of the OFAD Constraints and Distortion Polynomial," Memorandum, National Aeronautics and Space Administration, Goddard Space Flight Center, January 28, 1987
19. L. Abramowicz-Reed, "Procedure for Processing Data in the OTA Algorithms," Memorandum, Perkin-Elmer, March 9, 1987